Journal of Thermal Science and Technology

Vol. 5, No. 1, 2010

Thermodynamic Analysis of Expansion Profile for Displacement-type Expander in Low-temperature Rankine Cycle*

Mohd-Tahir MUSTHAFAH** and Noboru YAMADA**

**Graduate School of Energy and Environment Science, Nagaoka University of Technology, 1603-1 Kamitomioka-machi, Nagaoka-shi, Niigata 940-2188, Japan

E-mail: noboru@nagaokaut.ac.jp

Abstract

Thermodynamic analysis of the isentropic and polytropic expansion profiles of typical working fluids was carried out in order to design a highly efficient displacement-type expander for a low-temperature Rankine cycle. First, expansion profiles were analyzed for three typical working fluids: HFC245fa, ammonia, and supercritical CO_2. The hot-side temperature ranged from 60 ° to 120 °C, and the cold-side temperature was 10 °C. In the analysis, isentropic and polytropic expansion processes were assumed to behave thermodynamically. In the analysis results, we noted similarities among the expansion profiles for different hot-side temperatures. This similarity allowed us to introduce the unique concept of a variable mechanism for expansion profile fitting in displacement-type expanders. This variable expansion mechanism can be achieved by simply adjusting the position of the inlet and/or outlet port of the expander.

Key words: Organic Rankine Cycle, Thermodynamic Cycle, Thermal Efficiency, Expander Efficiency, Waste Heat Recovery, Displacement-type Expander

1. Introduction

In industries around the world, large amounts of low-temperature heat is wasted in internal combustion engines and other power sources. According to a report by the Energy Conservation Center of Japan[1], industrial waste heat is equivalent to approximately 70% of the yearly commercial and residential energy consumption in Japan. The report also mentions that the temperature level for 45% of the total waste heat is 100 °C and below. In automobiles, the waste heat with a temperature level around 100 °C makes up more than 60% of the heat generated by the fuel[2]. Therefore, it is important to develop an efficient waste heat recovery system to generate power from low-temperature heat sources with temperatures around 100 °C or less. In addition, the size of the recovery system must be fairly small because waste heat is a highly distributed energy source.

To generate power from the low-temperature difference between hot and cold heat sources, one of the most commonly used techniques is the organic Rankine cycle (ORC); a low boiling point organic fluid is used as a working fluid for the Rankine cycle. For example, Yamamoto et al.[3] described the effect of the thermal properties of an organic working fluid on the turbine power output of an ORC system. Freepower Co. Ltd. has introduced a commercial ORC system which converts waste heat into electricity[4]. Yamaguchi et al.[5] reported a unique Rankine cycle system that uses supercritical carbon

*Received 18 Nov., 2009 (No. 09-0699)
[DOI: 10.1299/jtst.5.61]

dioxide (CO_2) as the working fluid; they demonstrated their system's potential as a solar thermal energy conversion system. Almost all past research and development was carried out for power outputs far over 10 kW. For example, the turbine power outputs of the ORC systems developed by Ebara Co. Ltd.[6] and Free Power Co. Ltd. are approximately 12~15kW and 120 kW, respectively. ORC systems for low-temperature Rankine cycles with power outputs less than 10 kW have not yet been extensively studied and developed. However, the current global energy and environmental situation is such that compact low-temperature Rankine cycle systems will soon be required that can be easily installed at locations where waste heat is generated.

Compact low-temperature Rankine cycles have not been commonly implemented for actual low-temperature waste heat recovery because the thermal efficiency of systems implementing such cycles is low relative to its system cost; this is due to low efficiencies of an expander and a (working fluid) pump. Therefore, enhancing the thermal efficiency of the compact low-temperature Rankine cycle system is indispensable for practical applications. From our previous study in which several experiments were performed with regard to ORCs[7], we discovered that the expansion ratio of working fluids in the expander has a great impact on the expander efficiency, i.e., the system's thermal efficiency. When the working fluid expands in a displacement-type expander, the fluid should expand under an optimal volumetric expansion ratio, which changes according to the change in the temperature difference between the hot and cold sources. The volumetric expansion ratio of the expander, which is defined by the ratio of the discharge volume to suction volume in displacement-type expanders, should fit the appropriate working fluid's expansion ratio according to the heat source temperature difference, i.e., the temperature difference of working fluid between the expander inlet and outlet. In other words, to maintain high expander efficiency in a low-temperature Rankine cycle with a fluctuating heat source temperature, a variable expansion mechanism is required that can adjust the expansion ratio of the expander to the optimal expansion ratio of the working fluid for a given temperature difference.

However, there has been little research on such variable expansion mechanisms for displacement-type expanders in low-temperature Rankine cycle systems. To design a displacement-type expander with a variable expansion mechanism, the required optimal expansion profile of the working fluid must first be known; the expansion profile should fit the cell volume profile from the inlet (intake port) to the outlet (discharge port) of the displacement-type expander. Screw and scroll expanders[8][12] are two types of displacement-type expanders that are often employed in low-temperature Rankine cycle systems. In this study, we first analyzed the expansion profiles of three typical working fluids: HFC245fa (dry fluid), ammonia (wet fluid), and supercritical CO_2. The hot-side (expander inlet) temperature ranged from 60 to 120 °C, and the cold-side (expander outlet) temperature was 10 °C. In the analysis, isentropic or polytropic expansion processes was assumed to occur thermodynamically. Using the analysis results, we noted a similarity among the expansion profiles for different hot-side (expander inlet) temperatures. This similarity allowed us to introduce a conceptual variable mechanism to achieve the expansion profile fitting for a displacement-type expander. This variable expansion mechanism can be applied to the three typical working fluids analyzed in this study, and it can be achieved by simply adjusting the position of the inlet and/or outlet ports of the expander.

Nomenclature

$\dot{m}$	: Mass flow rate, kg/s
W	: Work, kJ/kg
h	: Enthalpy, kJ/kg
n	: Polytropic index
P	: Pressure, MPa
T	: Temperature, °C or K
$\dot{W}_P$	: Pump power, W
$\dot{W}_T$	: Turbine power, W
$\dot{Q}_C$	: Heat release at condenser, W
$\dot{Q}_E$	: Heat gain in evaporator, W
v	: Specific volume, m^3/kg

Subscripts

C	: Cold side (expander outlet)
E	: Hot side (expander inlet)
P	: Pump
T	: Turbine/Expander
WF	: Working fluid
Th	: Theoretical value

Greek symbols

η_{R_th}	: Theoretical thermal efficiency
η_T	: Expander efficiency

2. Rankine Cycle System

2.1 Outline of Rankine Cycle

Figure 1 shows a schematic of the operation principles for a conventional closed Rankine cycle. The ORC is a Rankine cycle that uses an organic working fluid. In this paper, we use the term "low-temperature Rankine cycle" or simply "Rankine cycle" instead of "organic Rankine cycle" because some of the working fluids that can be used are not regarded as organic matter, e.g., CO_2. The Rankine cycle consists of five main components: a pump, evaporator, expander, condenser, and working fluid. The evaporator and condenser are heat exchangers in the cycle that absorb and release heat.[8]. The cycle starts by the pump pushing the working fluid to the evaporator. In the evaporator, the hot-source water heats the working fluid up to the saturated or superheated vapor state. The vapor expands and rotates the expander to produce power. After the vapor leaves the turbine, the cold-source water cools and condenses the working fluid into the liquid state in the condenser. The pump then re-circulates the fluid. Figure 2 shows the pressure–enthalpy (p–h) diagram corresponding to Fig. 1.

Process 1→2 shown in Figs. 1 and 2 is the isentropic compression by the pump. The ideal pump power is given by

$$\dot{W}_P = \dot{m}_{WF}(h_2 - h_1) \quad (1)$$

Process 2→3 is the heating of the working fluid at a constant pressure in the evaporator. The heat absorbed by the working fluid is given by

$$\dot{Q}_E = \dot{m}_{WF}(h_3 - h_2) \quad (2)$$

Here, we define the hot-side temperature, i.e., expander inlet temperature T_E, as equivalent to the evaporating temperature of the working fluid in the evaporator.

Process 3→4 is the isentropic expansion in the expander. In an ideal Rankine cycle, expansion occurs without any heat losses, i.e., isentropic expansion; however, in actual systems, expansion tends to be a polytropic process. For isentropic expansion, the expander power is given by

$$\dot{W}_T = \dot{m}_{WF}(h_3 - h_4) \quad (3)$$

Process 4→1 is the cooling of the working fluid at a constant pressure in the condenser. The heat released from the working fluid is given by

$$\dot{Q}_C = \dot{m}_{WF}(h_4 - h_1) \quad (4)$$

Here, we defined the cold-side temperature, i.e., expander outlet temperature T_C, as equivalent to the condensing temperature of the working fluid in the condenser.

The theoretical thermal efficiency of the Rankine cycle is calculated as follows:

$$\begin{aligned}\eta_{R\_th} &= \frac{\text{Net power}}{\text{Total heat input}} \\ &= \frac{(\text{Expander power } \dot{W}_T) - (\text{Pump power } \dot{W}_P)}{\text{Heat gain in Evaporator } \dot{Q}_E} \\ &= \frac{(h_3 - h_4) - (h_2 - h_1)}{h_3 - h_2}\end{aligned} \quad (5)$$

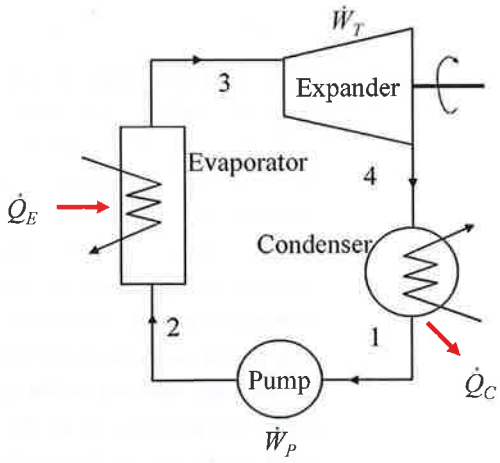

Fig.1 Schematic of closed Rankine cycle operation

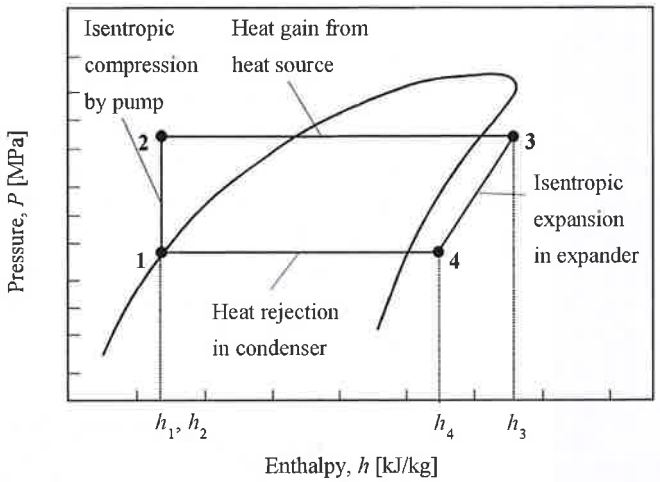

Fig.2 Pressure-enthalpy (p-h) diagram of closed Rankine cycle

The theoretical ideal expander power is calculated by the following equation:

$$\dot{W}_{T\_th} = \dot{m}_{WF}(h_3 - h_4) \tag{6}$$

The expander efficiency is calculated by the following equation:

$$\eta_T = \frac{h_3 - h_{4(calculate)}}{h_3 - h_{4(isentropic)}} \tag{7}$$

Here, $h_{4(calculate)}$ denotes the enthalpy at the expander outlet; it is calculated by assuming either isentropic or polytropic expansion processes. For an isentropic expansion process, η_T becomes unity (100%). In the abovementioned equations, the enthalpies and entropies were calculated by using the given pressure and temperature for each process. REFPROP ver. 8, which was developed by the NIST,[9] was used in the calculations.

3. Analysis of Volumetric Expansion Profile

3.1 Expansion Profile of HFC245fa

We analyzed the volumetric expansion profiles of three typical working fluids that can be used in recently developed low-temperature Rankine cycle systems. First, we present the details of the analysis results for HFC245fa, which is a "dry" fluid. We then show the results of two other working fluids: ammonia (NH_3), which is a "wet" fluid,[10] and supercritical CO_2. In the analysis, the hot-side (expander inlet) temperature T_E ranged from 60 to 120 °C. The cold-side (expander outlet) temperature T_C was constant at 10 °C. In addition, isentropic or polytropic expansion processes were assumed.

3.1.1 Expansion Profile Based on Isentropic Process

In an ideal Rankine cycle, the expansion process carried out by the expander is an isentropic process where no entropy change occurs. In the isentropic process, entropy does not change due to the internal reversible, adiabatic process of the working fluid expansion. Assuming an isentropic process, the specific volume of the working fluids can be theoretically calculated from the expander inlet to outlet conditions. To achieve isentropic expansion, the displacement-type expander should have a cell volume profile that is proportional to the calculated specific volume profile of the working fluid. Therefore, the calculated specific volume profile should let the expander satisfy the required optimal

expansion profile. Figure 3(a) shows a schematic diagram of an example model for a displacement-type expander. A rotary vane–type expander is used for the example because of its simple mechanism. Figure 3(b) shows the sample expansion profile corresponding to Fig. 3(a) represented by temperature. The calculation procedure of the expansion profile is as follows. Assume that the expander inlet condition (state point 3 in Fig. 2, position 1 in Fig. 3(a)) is in a saturated vapor state and that the expander inlet temperature T_E, enthalpy, entropy, pressure, and specific volume at the expander inlet are calculated. Then, using the same entropy at the expander inlet, the specific volumes at each given temperature (intervals of 5 K) are calculated until the temperature decreases T_C (state point 4 in Fig. 2, position 5 in Fig. 3(a)).

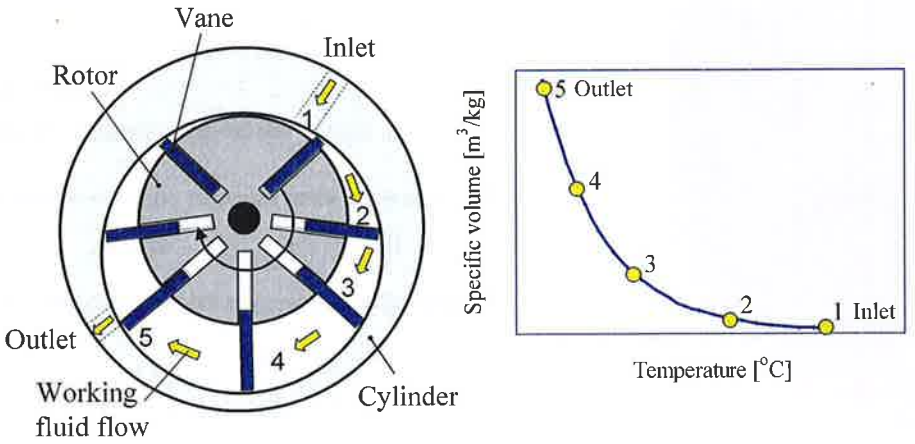

(a) Expansion in cell volume (b) Expansion profile corresponding to (a)

Fig.3 Example of displacement-type expander model used to explain the present analysis

3.1.2 Expansion Profile Based on Polytropic Process

In an actual expander, it is difficult to achieve the isentropic process described above. In a previous study, we performed experiments with a small ORC system[7]; we noticed that a polytropic process is usually observed in the actual working fluid expansion. Therefore, a polytropic process was assumed in addition to the isentropic process, and the results were compared with each other. The calculation procedure for an expansion profile based on a polytropic process is as follows. The enthalpy, pressure, and specific volume at the expander inlet are calculated in the same way as for the isentropic process. Specific volumes at given temperatures with intervals of 5 K are then calculated until the temperature decreases to T_C through the following well-known thermodynamic relationships for the polytropic process.

$$P_1 v_1 = P_2 v_2 \tag{8}$$

$$\frac{T}{P^{(n-1)/n}} = \text{constant} \tag{9}$$

Here, v denotes the specific volume of the working fluid. The polytropic index n was determined so that the expander efficiency was close to approximately η_T = 90%. Consequently, n = 1.08 was applied in the analysis. The resulting expander and thermal efficiencies are summarized in Table 1.

Table 1 Comparison of expander and thermal efficiencies for isentropic and polytropic expansion processes using HFC245fa

HFC245fa	ISENTROPIC		POLYTROPIC		
Hot-side temperature, T_E	Expander efficiency, η_T [%]	Thermal efficiency, $\eta_{R\ th}$ [%]	Polytropic index, n	Expander efficiency, η_T [%]	Thermal efficiency, $\eta_{R\ th}$ [%]
60 °C	100	14.2	1.08	89	12.8
80 °C	100	18.8	1.08	91	16.2
100 °C	100	21.3	1.08	93	19.1
120 °C	100	24.0	1.08	94	21.2

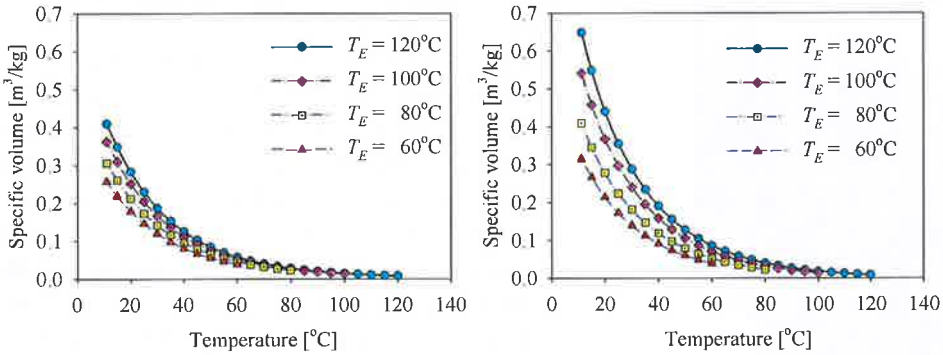

(a) Isentropic expansion (b) Polytropic expansion (n = 1.08)

Fig.4 Expansion profile of HFC245fa

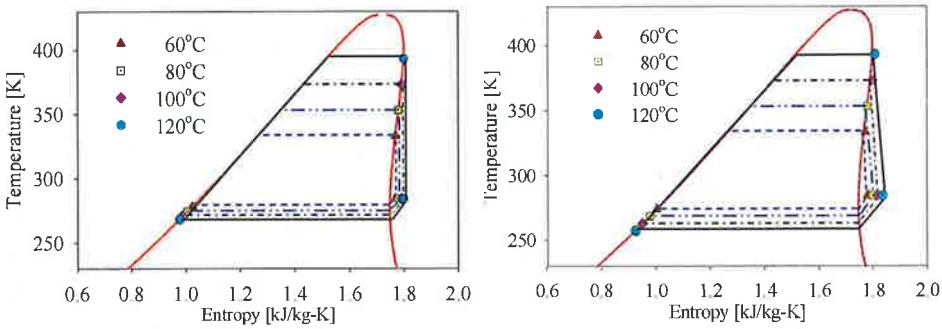

(a) Isentropic expansion (b) Polytropic expansion (n = 1.08)

Fig.5 Temperature-entropy (T-s) diagram for HFC245fa

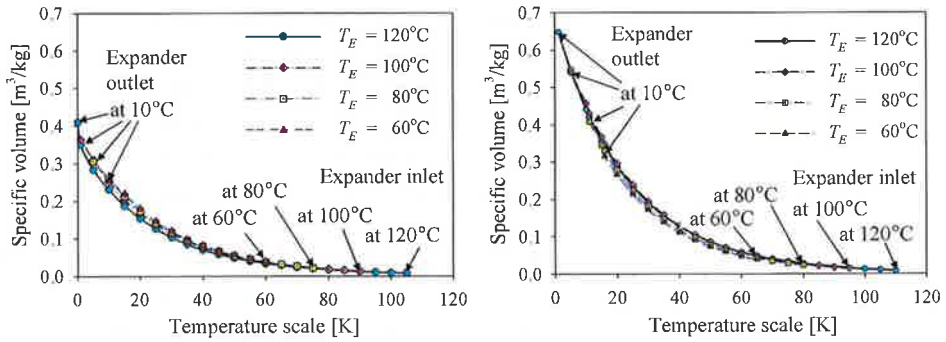

(a) Isentropic expansion (b) Polytropic expansion (n = 1.08)

Fig.6 Expansion profile fitting for HFC245fa

Shift amount and standard deviation for fitting profile are shown in Table 4.

3.1.3 Results and Expansion Profile Fitting

Figure 4 shows the expansion profile results for HFC245fa at T_E = 60, 80, 100, and 120 °C and T_C = 10 °C. Figures 4(a) and (b) shows the isentropic and polytropic expansion profile, respectively, at n = 1.08. The specific volume of the working fluid nonlinearly increased as the temperature of the working fluid decreased. The degree of this increase in specific volume was influenced by the temperature at which expansion began, i.e., the expander inlet temperature T_E. A larger T_E caused steeper expansion and resulted in a larger expansion ratio, which is defined here as the ratio of the specific volume at T_C to that at T_E. In polytropic expansion, the differences among the profiles for T_E tended to be larger than those for isentropic expansion. Clearly, the isentropic and polytropic expansion profiles were independent of each other according to the different expander inlet temperatures. Figures 5 (a) and (b) shows the temperature entropy (T-s) diagram corresponds to Fig.4(a) and Fig.4(b), respectively. In polytropic expansion (n=1.08), the entropy increases after the expansion, while the entropy does not change in isentropic expansion.

However, when comparing the curve shapes of the expansion profiles shown in Fig. 4, it seems that each curve could overlap each other and fit together in a single curve if we shift and adjust the horizontal axis of Fig. 4, i.e., the temperature axis. Figure 6 shows the results of the expansion profile fitting after shifting and adjusting only the horizontal axis of Fig. 4 to minimize the differences in specific volumes among all of the profiles. The shift amount of each profile and average standard deviation between each profile and the fitted profile in the overlapped range are shown in Table 4. Standard deviation is small and the maximum difference in specific volume is within 0.032 and 0.029 m^3/kg for isentropic and polytropic expansion, respectively. The horizontal axis in Fig. 6, which is the "temperature scale," represents relative values in units of K. Clearly, the profiles almost fit together. This is a key feature that led us to develop the variable expansion concept described below.

3.2 Concept of Variable Expansion

The fitting curve shown in Fig. 6 led us to a unique concept: an expander with the same cell volume profile as this fitting curve can be used for a wide range of T_E conditions, i.e., for a wide range in temperature differences between the hot-side (expander inlet) and cold-side (expander outlet) temperatures. This means that a single expander can be used for different heat source temperature levels by simply adjusting the starting position for expansion, i.e., the cell volume at the expander inlet (intake port) depending on the T_E and/or T_C level. Consequently, the volumetric expansion ratio of the expander can be optimally controlled for fluctuations in the temperature difference. In Fig. 6, the preferred positions for the expander inlet at several T_E levels are indicated. The expander outlet position also can be adjusted if the cold-side temperature level fluctuates.

We expect that the present concept is more feasible for displacement-type expanders rather than velocity-type expanders because the cell volume profile of the former can be designed mechanically, while the profile of the latter has to be designed with consideration for thermofluid dynamics. The screw expander is a candidate displacement-type expander in which the variable expansion concept can be effectively applied, although we do not go into further detail of the variable mechanism for the screw expander in this paper. This concept helps contribute to the thermal efficiency of low-temperature Rankine cycles exposed to heat source temperature fluctuations; this is because mismatches of the volumetric expansion ratio, which cause a drastic decline in expander efficiency, are solved by the variable expansion concept. For example, in case of the isentropic expansion shown in Table 1, Fig.4(a), and Fig.5(a), if the expansion ratio decreases to 46% of ideal expansion ratio (i.e., the ratio achieving η_T = 100%) for each T_E = 60, 80, 100, and 120 °C, then the expander efficiency theoretically reduces to η_T = 79%, 75%, 70% and 60%, respectively. Actually, according to our previous experiment[8], the expander efficiency decreased from

η_T = 92% to 52% when the volumetric expansion ratio decreased to 49% of the optimal ratio.

3.3 Analysis of Other Working Fluids

For the expansion profile analysis, the other two working fluids—supercritical CO_2 and NH_3—were selected because they are currently used for Rankine cycle systems. The expansion profiles were calculated and observed under the conditions of a hot-side temperature ranging from T_E = 60 to 120 °C and a cold-side temperature at T_C = 10 °C. The results for supercritical CO_2 and NH_3 show that the expansion profile fitting is successful for both working fluids as well as HFC245fa. Therefore, this study shows that the proposed concept of a variable expansion mechanism can be applied to at least three working fluids for the given temperature range.

3.3.1 Supercritical CO_2

The same abovementioned method was used to analyze the isentropic and polytropic profiles for supercritical CO_2. For a supercritical CO_2 Rankine cycle, the evaporating and condensing pressures must be given explicitly. Zhang et al.'s experimental data[11] were used as a reference. Evaporating pressures of 8.0, 10.2, 12.9, and 16.3 MPa were given for T_E = 60, 80, 100, and 120 °C, respectively. To calculate the polytropic profile, the polytropic index n was determined so that the expander efficiency ranged between 70%–90%. On the basis of these results, n = 1.29 was applied to the analysis.

Figures 7 and 8 show the expansion profiles and T-s diagram, respectively, for supercritical CO_2. The differences in curve shapes for the profiles were smaller than those for HFC245fa, although the expander and thermal efficiencies in the polytropic profile were lower than those in the isentropic profile, as shown in Table 2. Expansion profile fitting was performed, and a similar result as that obtained in the HFC245fa analysis was observed, as shown in Fig. 9. The curve shapes of the expansion profiles fitted each other well when we adjusted the horizontal axis. The shift amount and standard deviation between each profile and the fitted profile are shown in Table 5. The maximum difference of the specific volume was within 0.005 m^3/kg for both the isentropic and polytropic expansion profiles.

3.3.2 Ammonia (NH_3)

NH_3 was selected for analysis as a representative wet fluid. A combined thermal power and cooling cycle using NH_3 as the working fluid has been reported[13]. We assumed a superheating cycle for which we needed to give not only the evaporating temperature but also the evaporating pressure. Evaporating pressures of 1.2, 1.5, 1.9, and 2.4 MPa were given for T_E = 60, 80, 100, and 120 °C, respectively. Using the same method as for HFC245fa, the NH_3 expansion profiles were obtained. For polytropic expansion, the polytropic index n was determined so that the expander efficiency was between 80 and 90%. Consequently, n = 1.2 was applied for the analysis.

Figure 10 shows the expansion profiles of NH_3. The isentropic profiles showed a good curve fitting feature without the fitting adjustment, while polytropic profiles showed differences among the profiles. Figure 11 is the T-s diagram for both isentropic and polytropic expansion. Figure 12 shows the fitting profile after the fitting adjustment. The shift amount and standard deviation between each profile and the fitted profile are shown in Table 6. The maximum difference in specific volume was within 0.001 and 0.01 m^3/kg for the isentropic and polytropic expansion profiles, respectively.

Table 2 Comparison of expander and thermal efficiencies for isentropic and polytropic expansion processes using CO_2

CO_2	ISENTROPIC		POLYTROPIC		
Hot-side temperature, T_E	Expander efficiency, η_T [%]	Thermal efficiency, $\eta_{R\ th}$ [%]	Polytropic index, n	Expander efficiency, η_T [%]	Thermal efficiency, $\eta_{R\ th}$ [%]
60 °C	100	9	1.29	66	4.8
80 °C	100	11	1.29	73	7.3
100 °C	100	14	1.29	80	10.4
120 °C	100	17	1.29	87	13.9

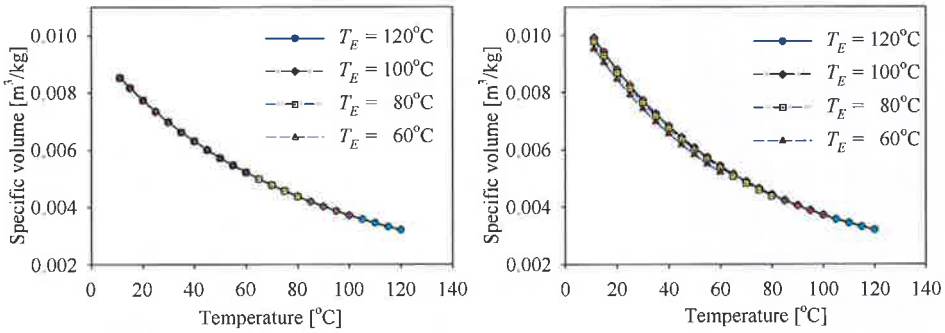

(a) Isentropic expansion (b) Polytropic expansion (n = 1.29)

Fig.7 Expansion profile of supercritical CO_2

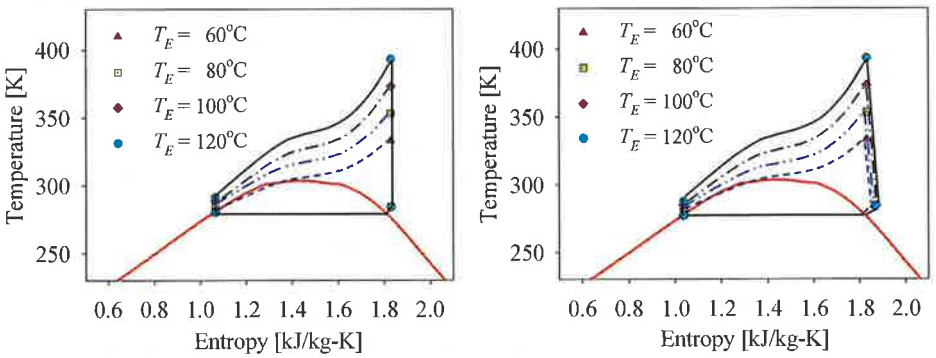

(a) Isentropic expansion (b) Polytropic expansion (n = 1.29)

Fig. 8 Temperature-entropy (T-s) diagram for CO_2

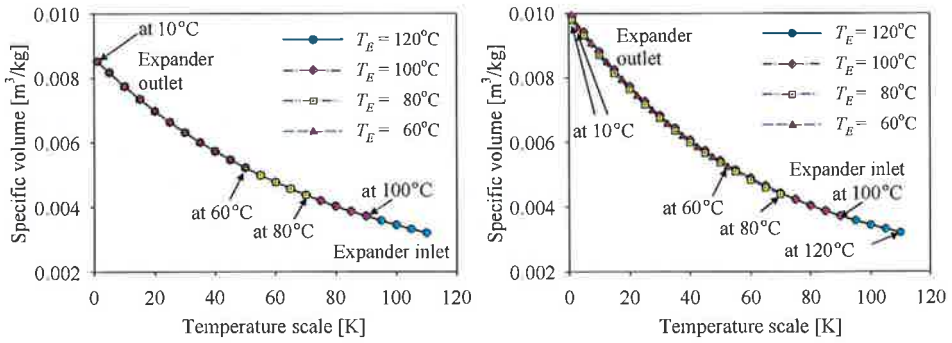

(a) Isentropic expansion (b) Polytropic expansion (n = 1.29)

Fig.9 Expansion profile fitting for CO_2 profile

Shift amount and standard deviation for fitting profile are shown in Table 5.

Table 3 Comparison of expander and thermal efficiencies for isentropic and polytropic expansion processes using NH_3

NH_3	ISENTROPIC		POLYTROPIC		
Hot-side temperature, T_E	Expander efficiency, η_T [%]	Thermal efficiency, $\eta_{R\ th}$ [%]	Polytropic index, n	Expander efficiency, η_T [%]	Thermal efficiency, $\eta_{R\ th}$ [%]
60 °C	100	7.1	1.2	87.8	6.1
80 °C	100	9.7	1.2	88.8	8.4
100 °C	100	12.2	1.2	89.7	10.5
120 °C	100	14.6	1.2	90.4	12.6

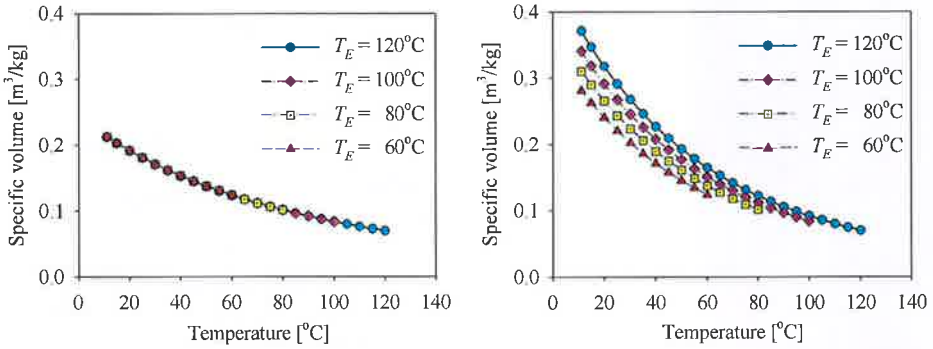

(a) Isentropic (b) Polytropic (n = 1.2)

Fig.10 Expansion profile of NH_3

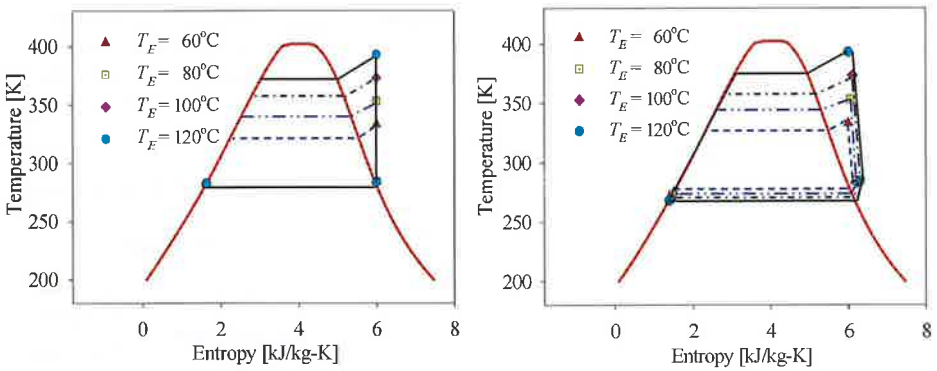

(a) Isentropic (b) Polytropic (n = 1.2)

Fig.11 Temperature-entropy (T-s) diagram for NH_3

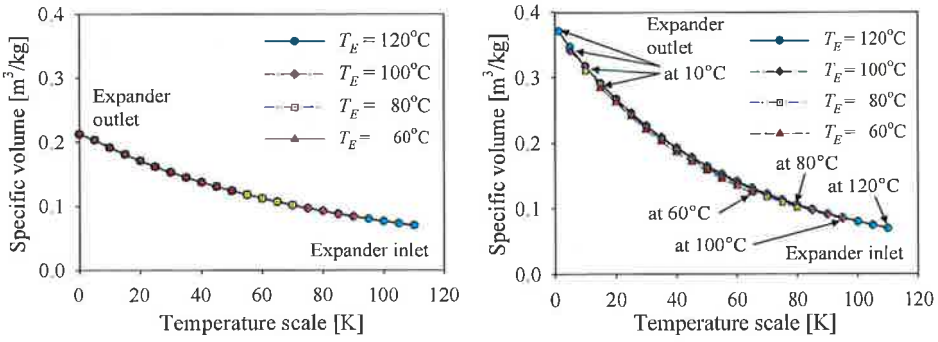

(a) Isentropic expansion (b) Polytropic expansion (n = 1.2)

Fig.12 Expansion profile fitting for NH_3

Shift amount and standard deviation for fitting profile are shown in Table 6.

Table 4 Detail of expansion profile fitting for HFC245fa

Profile in Fig.6	Isentropic		Polytropic	
	Shift from original profile	Standard deviation	Shift from original profile	Standard deviation
T_E= 60°C	0K	5.6×10^{-5}	+5K	1.3×10^{-4}
T_E= 80°C	-5K	2.5×10^{-5}	0	1.3×10^{-5}
T_E= 100°C	-9K	8.4×10^{-7}	-5K	9.4×10^{-5}
T_E= 120°C	-10K	1.3×10^{-4}	-10K	3.2×10^{-5}

Table 5 Detail of expansion profile fitting for CO_2

Profile in Fig.9	Isentropic		Polytropic	
	Shift from original profile	Standard deviation	Shift from original profile	Standard deviation
T_E= 60°C	-10K	1.1×10^{-8}	-7.5K	3.7×10^{-8}
T_E= 80°C	-10K	1.0×10^{-9}	-10K	4.5×10^{-9}
T_E= 100°C	-10K	2.1×10^{-9}	-10K	1.6×10^{-9}
T_E= 120°C	-10K	1.1×10^{-9}	-10K	8.0×10^{-9}

Table 6 Detail of expansion profile fitting for NH_3

Profile in Fig.12	Isentropic		Polytropic	
	Shift from original profile	Standard deviation	Shift from original profile	Standard deviation
T_E= 60°C	-10K	1.1×10^{-9}	+5K	1.8×10^{-5}
T_E= 80°C	-10K	1.0×10^{-8}	0	5.1×10^{-7}
T_E= 100°C	-10K	1.2×10^{-9}	-5K	3.1×10^{-6}
T_E= 120°C	-10K	1.1×10^{-9}	-10K	9.4×10^{-6}

4. Conclusions

In this study, thermodynamic analysis was carried out to analyze the isentropic and polytropic expansion profiles of HFC245fa, supercritical CO_2, and NH_3 for the design of a highly efficient displacement-type expander for low-temperature Rankine cycles. The following results were obtained:

1) Expansion profiles of the selected working fluids varied depending on the temperature difference between the hot-side and cold-side temperatures; in this study, the hot-side temperature ranged from 60 to 120 °C, and the cold-side temperature was 10 °C. The Polytropic expansion profiles showed larger differences at various hot-side temperature levels.
2) Despite the differences in the expansion profiles, a similarity in the curve shapes of each expansion profile was observed. Exploiting this similarity, profile fitting was carried out; as a result, every expansion profile fit each other well enough to be regarded as one profile. Based on this fact, the unique concept of a variable expansion mechanism is proposed in this paper.
3) The proposed variable expansion mechanism can potentially maintain a high expander efficiency for displacement-type expanders by controlling the volumetric expansion ratio of the expander; this can be achieved by simply adjusting the expander inlet and/or expander outlet positions, even when the temperature difference between the hot-side and cold-side temperatures fluctuates. The higher expander efficiency results in a higher thermal efficiency for low-temperature Rankine cycles.

References

[1] Nasu, H., Waste heat quantity assumption from overall Japan industries, *Press Release of Energy Conservation Center of Japan* (in Japanese), August 12, (1997), (online) available from <http://www.eccj.or.jp/press/scw990812.html>, (accessed 2009-08-20).

[2] Ibaraki, S., Endo, T., Kojima, Y., Takahashi, K., Baba, T. and Kawajiri, S., Study of efficient on-board waste heat recovery system using Rankine cycle, *Japan Society of Automotive Engineers*, Vol. 28, (2007), pp. 307–313.

[3] Yamamoto, T., Furuhata, T., Arai, N. and Mori, K., Design and testing of the organic Rankine cycle, *Energy*, Vol. 26, (2001), pp. 239–251.

[4] Freepower, "Introduction to Freepower ORC systems," June, (2005), (http://www.freepower.co.uk).

[5] Yamaguchi, H., Zhang, X. R., Fujima, K., Enomoto, M. and Sawada, N., Solar energy powered Rankine cycle using supercritical CO_2, *Applied Thermal Engineering*, Vol. 26, (2006), pp. 2345–2354.

[6] Inoue, N., Takeuchi, T., Kaneko, A., Uchimura, T., Irie, K. and Watanabe, H., Development of Electric Power Units Driven by Waste Heat, *JSRAE (in Japanese)*, Vol. 22, (2005), pp. 357–368.

[7] Musthafah, M. T., Yamada, N., Characteristics of small ORC system for low temperature waste heat recovery, *JSME, Journal of Environment and Engineering*, Vol. 4, (2009), pp. 375–385.

[8] Saitoh, T., Yamada, N. and Wakashima, S.-I., Solar Rankine cycle system using scroll expander, *JSME, Journal of Environment and Engineering*, Vol. 2, (2007), pp. 708–719.

[9] NIST, "Reference Fluid Thermodynamic and Transport Properties Database (REFPROP) Version 8.0," U.S. Department of Commerce, Maryland, (2002).

[10] Badr, O., O'Callaghan, P. W. and Probert, S. D., Selecting A Working Fluid for a Rankine-cycle Engine, *Applied Energy*, Vol. 21, (1985), pp. 1–42.

[11] Zhang, X. R., Yamaguchi, H., Fujima, K., Enomoto, M. and Sawada, N., Theoretical analysis of a thermodynamic cycle for power and heat production using supercritical carbon dioxide, *Energy*, Vol. 32, (2007), pp. 591–599.

[12] Badr, O., Naik, S., O'Callaghan, P. W. and Probert, S. D., Expansion machine for a low power-output steam Rankine-cycle engine, *Applied Energy*, Vol. 39, (1991), pp. 93–116.

[13] Tamm, G., Goswami, D.Y., Lu, S. and Hasan, A.A., Theoretical and experiment investigation of an ammonia-water power and refrigeration thermodynamic cycle, *Solar Energy*, Vol. 76, (2003), pp. 217–228.